Heliyon 8 (2022) e10489

Contents lists available at ScienceDirect

Heliyon

journal homepage: www.cell.com/heliyon

Research article

Removal of arsenic in groundwater from western Anatolia, Turkey using an electrocoagulation reactor with different types of iron anodes

Mehmet Kobya [a,b], Mustafa Dolaz [b,c], Burcu Özaydın-Şenol [a], Aysegul Yagmur Goren [d,*]

[a] Gebze Technical University, Department of Environmental Engineering, 41400, Kocaeli, Turkey
[b] Kyrgyz-Turkish Manas University, Department of Environmental Engineering, Bishkek, Kyrgyzstan
[c] Kahramanmaraş Sütcü İmam University, Department of Environmental Engineering, 46040, Kahramanmaraş, Turkey
[d] Izmir Institute of Technology, Department of Environmental Engineering, İzmir, Turkey

ARTICLE INFO

Keywords:
Arsenic removal
Electrocoagulation
Groundwater
Ball anode
Scrap anode
Plate anode

ABSTRACT

Electrocoagulation (EC) is a significantly efficient method for As removal from waters and received considerable attention recently. In this study, the natural groundwater (GW) samples containing As concentrations of GW-1: 538.8 μg L^{-1}, GW-2: 1132.1 μg L^{-1}, and GW-3: 52, 000 μg L^{-1} were obtained from different provinces and treated by EC process using different iron anodes (plate, ball, and scrap). To achieve drinking water As standard (10 μg L^{-1}), the operational time, applied current, and As removal optimization for all anode types were studied. At applied current of 0.025 A, the As removal efficiency, EC time, and operating cost were >99.9%, 180 min and 0.406 $ m^{-3} for ball anodes, >99.9%, 100 min and 0.0813 $ m^{-3} for plate anodes, >99.9%, 80 min and 0.0815 $ m^{-3} for scrap anodes for GW-3, respectively. It was observed that as the As concentration in the GW increased, the EC time and operating cost increased. Overall, it was concluded that Fe scrap anodes are more advantageous than other types of anodes in terms of operating cost in EC reactor for As removal.

1. Introduction

After the World Health Organization's (WHO) new revision on arsenic (As) in 1993, it has been announced as a major problem related to arsenic pollution in natural water resources all over the world (Nordstrom, 2015; WHO, 2001). Recently, the groundwater resources in countries such as West Bengal, India, Bangladesh, Cambodia, Canada, China, Argentina, Chile, Mexico, Nepal, Taiwan, Turkey, USA, and Vietnam have been facing As contamination at concentrations above 50 μg L^{-1} (Choong et al., 2007; Ravenscroft et al., 2009). High As concentrations of 10-10, 700 μg L^{-1} in groundwater resources have been reported in many parts of Turkey, especially in Western Anatolia (Gunduz et al., 2010, 2017; Gemici et al., 2008; Dogan and Dogan, 2007; Colak et al., 2003). The accumulation and mobilization of As in groundwater widely resulted from water-rock interactions and the geochemical structure of the environment (Smedley and Kinniburgh, 2002). To protect public health against the harmful effects of As, the US Environmental Protection Agency (US-EPA) and the World Health Organization (WHO) decreased the permissible level for As in drinking water from 50 to 10 μg L^{-1} (US-EPA, 2016; WHO, 2001).

Chronic effects of As exposure via drinking water include skin lesions and cancers, cardiovascular disease, diabetes mellitus, internal organ cancers, hypertension, neurological effects, and respiratory disease (Choong et al., 2007; Çöl and Çöl, 2004; Çolak et al., 2003). Moreover, in waters, As exists mainly in inorganic forms such as arsenite (III) and arsenate (V). As (V) dominates in oxygenated waters, As (III) dominates in more reducing environments (Smedley and Kinniburgh, 2002). The mobility and toxicity of As (III) were also higher than that of the As (V) (Bordoloi et al., 2013). Considering toxic health effects and chemical forms of As in natural water resources is urgent to treat by a simple, feasible method, and cost-effective groundwater to supply safe drinking water. At this point, the US-EPA has identified seven technologies as the best available technologies (BATs) and their As removal efficiency; (1) ion-exchange (95%), (2) alumina (95%), (3) reverse osmosis (>95%), (4) coagulation/filtration (95%), (5) lime softening (90% at pH > 10.5), (6) electro dialysis (85%), and (7) oxidation/filtration (80% at 20:1 of Fe:As ratio) (US-EPA, 2000). However, to enhance total As removal, the oxidation of As (III) to As (V) is necessary prior to processes such as coagulation, adsorption, and ion exchange. In addition, these As removal processes have many disadvantages with the addition of treatment

* Corresponding author.
E-mail address: yagmurgoren@iyte.edu.tr (A.Y. Goren).

https://doi.org/10.1016/j.heliyon.2022.e10489
Received 28 March 2022; Received in revised form 19 April 2022; Accepted 25 August 2022

chemicals and require a pre-oxidation process. This creates prolonged treatment time, extended operational complexity, high operating costs, and large volumes of sludge and secondary pollutants.

Recently, As removal efficiency as high as >99% through the electrocoagulation (EC) process has been reported for many drinks of water and wastewaters (Song et al., 2017; Kobya et al., 2017; Alcacio et al., 2014; Amrose et al., 2013; Molgora et al., 2013; Vasudevan et al., 2010; Parga et al., 2005). In the EC process, Electrochemical dissolution of sacrificial metal electrodes generates metallic hydroxide flocks within the water. Even, in water, soluble elements, organic compounds, and colloidal pollutants generate a variety of coagulated forms and metal hydroxides, which destabilize and agglomerated particles or co-precipitate and adsorb soluble pollutants. EC process is an efficient and alternative process for As removal owing to its significant benefits such as no need for additional chemicals for oxidation of As (III) to As (V), pH adjustment, low operational time, high treatment performance, ease of operation and maintenance, and relatively cost-effective (Parga et al., 2005). At the same time, the process conditions (i.e., applied current or current density, time of processing, pH, arsenic concentration in water sample), the shape of the reactor, shape (i.e., plate, rod, ball, scrap), and type (Fe, Al) of electrodes are affecting the performance of the EC process. Since sacrificial metal anodes in the EC process are usually used of iron and aluminum plates, these electrodes have a relatively low surface area and high manufacturing costs, making EC technology economically impractical. On the other hand, the waste-scrap electrodes have a larger surface area than the other two-dimensional electrodes, thus presenting a significant contact are between the contaminants and anodes in EC reactor, enhancing the practical application of EC process owing to its low cost (Vignesh et al., 2017; Elazzouzi et al., 2021). Moreover, even the available literature studies on arsenic removal by EC process using a plate, ball, and scrap electrodes are generally synthetically prepared As solutions, and very limited studies with real As-contaminated groundwater samples have been performed (Kobya et al., 2015, 2017; Amrose et al., 2013; Garcia-Lara and Montero-Ocampo, 2010). Hence, the EC technology using a different type of iron anodes for As removal from groundwater needs to be further studied and considered.

In this paper, As removal from real groundwater samples using two different EC reactors with three types of iron anodes (plate, ball, and scrap) was investigated. Effects of operational parameters such as current and operational time on As removal efficiency was also determined for all anodes, and the optimum operating conditions were investigated. The operating costs for treated groundwater samples and all anode types were calculated to give an insight into the economic feasibility of the technology.

2. Arsenic removal mechanism by EC

In the EC method with iron anodes, the iron ions (Fe^{2+} and Fe^{3+}) are generated at the surface of the iron anode (Eqs. (1) and (2)); hydrogen gas is also released at the cathode (Eq. 3). The release of $H_{2(g)}$ helps to mix the flocculated particles in water (Amrose et al., 2013).

Anode electrode:

$$Fe \rightarrow Fe^{2+} + 2e^{-} \quad \text{Eq. 1}$$

$$Fe^{2+} \rightarrow Fe^{3+} + e^{-} \quad \text{Eq. 2}$$

Cathode electrode:

$$2H_2O + 2e^{-} \rightarrow H_{2(g)} + 2OH^{-} \quad \text{Eq. 3}$$

At the same time, the rate of oxidation of Fe^{2+} depends on dissolved oxygen in the solution (Eq. 4).

$$O_{2(g)} + 4Fe^{2+} + 2H_2O \rightarrow 4Fe^{3+} + 4OH^{-} \quad \text{Eq. 4}$$

Electrolytic oxidation of iron anode in the EC process generates hydrous ferric oxides (HFeO; also called Fe^{3+} precipitates) such as goethite, lepidocrocite, hematite, maghemite, or magnetite in As contaminated water. The generated Fe^{3+} ions react with hydroxyl ions in the solution to originate amorphous HFeO flocks depending on the pH of the solution. Contaminants such as form complexes with HFeO and then these aggregates can be removed in water. As a result, the As removal mechanism is related to the formation of HFeO due to coagulation, co-precipitation, electro-oxidation, and precipitation. In groundwater at neutral pH are the predominant arsenate species such as $HAsO_4^{2-}$ and $HAsO_4^{-1}$. The main mechanism of As removal is by adsorption reaction, in which HFeO flocks adsorb the arsenate ion (Eqs. 5, 6, and 7). A generation of dark green iron oxyhydroxides flocks defines visually the success of As removal (Sık et al., 2017; Banerji and Chaudhari, 2016; Moreno et al., 2009).

$$mFe^{3+} + (3m-n)OH^{-} + nHAsO_4^{2-} \rightarrow Fe_m(OH)_{(3m-n)}(HAsO_4)_{n(s)} \quad \text{Eq. 5}$$

$$3FeOOH_{(s)} + HAsO_4^{2-} \rightarrow (FeO)_3AsO_{4(s)} + H_2O + 2OH^{-} \quad \text{Eq. 6}$$

$$2FeOOH_{(S)} + H_2AsO_4^{-} \rightarrow (FeO)_2HAsO_{4(S)} + H_2O + OH^{-} \quad \text{Eq. 7}$$

Where (s) is solid phase and (m) and (n) are the stoichiometric coefficients depending on the reaction conditions.

3. Material and methods

3.1. Characterization of natural groundwater samples

The As problem in groundwater and surface waters in Emet, Hisarcik, and Tavşanli in Districts of Kütahya Province and Bigadiç in Balikesir Province (Turkey) has been reported in literature studies (Çöl and Çöl, 2004; Dogan et al., 2005; Dogan and Dogan, 2007). The area surrounding colemanite mines (Emet and Hisarcik in Kütahya; Bigadiç in Balikesir) and silver mining (Kütahya, Tavşanli) shows extremely high As contamination in groundwater (<10-10,700 μg L^{-1}). Therefore, in this study, high As containing groundwater samples (GWs) were collected from wells and springs located at Kütahya and Balikesir Provinces in the western Anatolia part of Turkey. Three different natural groundwater sample were obtained from Dulkadir Village (Kütahya province, Tavşanlı) near the silver mining operation (GW-1), Yukari Yoncaağaç Village (Kütahya province, Hisarcik) near Hisarcik open-pit colemanite mine (GW-2), and from a well in the open pit colemanite mining operation in Bigadiç (Balıkesir province) (GW-3). The relevant water quality parameters of studied GWs are presented in Table 1.

3.2. EC reactors set-up and experimental procedure

Two different types of EC reactors were used for As removal experiments. The set-up of rectangular (Figure 1a) and cylindrical-shaped plexiglass EC reactors (Figure 1b) are documented in detail in our previous studies (Kobya et al., 2015; Goren and Kobya, 2021). Ball, scrap, and plate-type iron electrodes were obtained from a metal machining shop. For the experimental procedure, 0.94 L of groundwater sample was fed into the EC reactors. The four iron plate electrodes (two anodes + two cathodes) with dimensions 50 mm × 73 mm x 3 mm were placed in the rectangular EC reactor, while the cylindrical-shaped reactor was filled with iron balls of 5 mm diameter or iron scraps of 1.8–15 mm long and 0.50–3.0 mm wide. The voltage measurement and current supply were carried out with a direct current (DC) power supply (Agilent 6675A model; 120V, 18A). The current was adjusted to the desired value in the DC power supply for each experiment. Furthermore, an air-fed diffuser was utilized for the aeration of the cylindrical-shaped reactor. The samples were taken from the reactors at selected time intervals for analysis. Prior to As analyses, samples were filtered through a 0.45 μm membrane filter. Moreover, the anode electrodes at the end of each experimental run are washed thoroughly with distilled water, dried, and weighted. All experimental runs were performed at the temperature of 20 ± 2 °C under different current density values.

Table 1. Physicochemical parameters and chemical composition of groundwater samples.

Parameters	GW-1	GW-2	GW-3
Temperature (°C)	23.4 ± 0.01	23.4 ± 0.01	23.4 ± 0.01
pH (-)	8.11 ± 0.18	7.59 ± 0.04	6.85 ± 0.04
Electrical conductivity (mS cm^{-1})	0.43 ± 0.04	1.44 ± 0.05	6.0 ± 0.13
Total dissolved solids (TDS, mg L^{-1})	358 ± 2.00	1200 ± 5.03	5010 ± 2.65
Dissolved oxygen (DO, mg L^{-1} O_2)	6.9 ± 0.12	5.2 ± 0.10	7.2 ± 0.02
Dissolved organic carbon (DOC, mg L^{-1})	3.1 ± 0.19	2.7 ± 0.02	1.3 ± 0.03
Total alkalinity (mg $CaCO_3$ L^{-1})	240 ± 4.58	350 ± 1.00	900 ± 7.0
Total hardness (mg $CaCO_3$ L^{-1})	21.6 ± 0.20	78.1 ± 0.22	450 ± 2.0
Sulphate (mg SO_4 L^{-1})	56.8 ± 0.02	72.5 ± 0.31	82.2 ± 0.1
Nitrate (mg NO_3–N L^{-1})	7.7 ± 0.05	9.4 ± 0.05	10.8 ± 0.05
Chloride (mg Cl L^{-1})	8.4 ± 0.02	12.3 ± 0.07	11.6 ± 0.06
Phosphorus (mg L^{-1})	0.11 ± 0.02	0.20 ± 0.01	0.10 ± 0.01
Boron (mg L^{-1})	2.8 ± 0.01	6.4 ± 0.02	38.5 ± 0.07
Iron (mg L^{-1})	0.64 ± 0.04	0.26 ± 0.01	0.11 ± 0.01
Manganese (mg L^{-1})	0.15 ± 0.01	0.09 ± 0.01	0.10 ± 0.02
Total arsenic (μg L^{-1})	538.8 ± 0.01	1132 ± 1.64	52,000 ± 1.99

3.3. Analytical methods

The analyses of GWs were performed using standard methods (APHA, 1998). As, iron, magnesium and boron concentrations were measured with an inductively coupled plasma optical emission spectrometer (ICP-OES, PerkinElmer Optima 7000 DV model). The ICP-OES calibration is very essential before analysis to get an accurate value. The instrument was calibrated with the help of As stock solution (ICP Standard, Merck Certipur®, Germany) by preparing a calibration curve and reference solutions for freshly prepared stock solution. Similarly, the calibration curves were constructed using a series of dilutions containing different levels of heavy metals using standard solutions. The instrument detection limits were estimated by taking 10 replicate measurements of the calibration blank (1% nitric acid). The detection limits were calculated as < 0.01, 0.2, 0.1, and 1.1 μg L^{-1} for As, iron, magnesium, and boron respectively. The readings were made at the emission wavelengths for As, iron, magnesium, and boron of 193.691, 259.933, 279.071, and 249.672 nm, respectively. After calibration, the initial performance solution was performed (for all analytes at the levels of their respective standards) and the recoveries were found as 100, 96, 92, and 98% for As, iron, magnesium, and boron, respectively. The precision values (%RSD) were also monitored to ensure the short-term stability of emission signals and the precision values were 2.1, 1.2, 1.5, and 0.2% for As, iron, magnesium, and boron, respectively. Anions (chloride, nitrate, phosphorus and sulfate) were determined by ion chromatography (IC, Shimadzu HIC-20A). The dissolved organic carbon (DOC) content of samples was determined using a non-dispersive IR source (Shimadzu, TOC-L model, Japan) by the non-purgeable organic carbon method. The pH, dissolved oxygen (DO) and total dissolved solids (TDS) were measured using a pH meter (Hach Lang HQ40d model), and the conductivity was determined with a conductivity meter (Mettler Toledo SG3 model). All chemicals were analytical grade. All analytical measurements were carried out with three replicates and averaged data were used. Standard deviation values were between 0.01 and 1.99 μg L^{-1} for As and 0.005 and 7 mg L^{-1} for other parameters (Table 1). The experimental error was <2% for all runs. Moreover, the As adsorption capacities were calculated using average values. Therefore, the As adsorption capacity values have no standard deviation.

3.4. Statistical analysis

The normality and homogeneity of variance of the associated water quality parameter values were tested by the Shapiro-Wilk test and Levene tests, respectively. The results of the Shapiro-Wilk test showed that all parameters were normally distributed with p-vale < 0.05. The Levene test results revealed that the water quality parameters variances were not significantly different except DOC in GW-2, hardness in GW-1, boron, iron, and As in all GWs with p-vale > 0.05. Furthermore, these statistical analyses were followed by an ANOVA-One-Way test to identify significant differences between GWs. For all water quality parameters, the ANOVA test showed that the means are significantly different (p-value < 0.05).

Moreover, the differences between the anode materials considering As removal performance in different GW sources were determined using a Kruskal-Wallis test. The test results revealed that the As removal performance of anode materials was significantly different for GW-1 and GW-2 samples with a p-value < 0.05, while it was not significantly different for GW-3 with a p-value >0.05. The tests result also showed that the As removal performance of ball, scrap, and plate anode materials

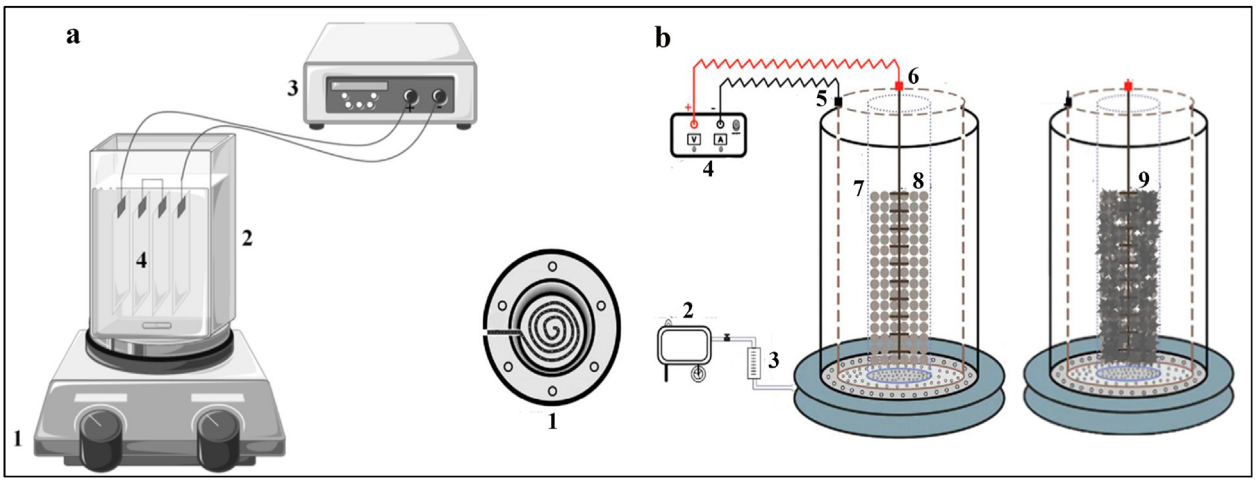

Figure 1. Experimental set-up of rectangular EC reactor **(a)**: (1) Magnetic stirrer, (2) Rectangular reactor, (3) DC power supply, (4) Fe plate electrodes and cylindrical-shaped EC reactor **(b)**: (1) Air-fed diffuser, (2) Compressor, (3) Flow mater, (4) DC power supply, (5) Titanium cathode, (6) Supporting rod, (7) Inner cylinder, (8) Fe ball electrodes, (9) Fe scrap electrodes.

were significantly different at 0.05 level (p-value < 0.05). In addition, the As removal performance of the ball, plate, and scrap anode materials were statistically analyzed by the Mann-Whitney U test. The As removal performance of scrap anode was greater (p-value < 0.05) in all GWs than plate and ball anodes. On the other hand, the removal performance of the plate anode was more excellent (p-value <0.05) compared with the ball anode.

4. Results and discussion

4.1. Effect of applied current on as removal

The most important parameter affecting As removal efficiency of the EC process is the applied current or current density (Shen et al., 2022). Applied current (*i*) or current density in the EC process determines coagulant (electrochemically dissolved iron ions) dosage rate, bubble production rate, flocs size, and growth rate (Kobya et al., 2015; Amrose et al., 2013). According to Faraday's law, the charge passed to the solution is directly proportional to the amount of metallic iron electrode (Fe) dissolved; meaning that As removal by the EC is governed by the formation of iron oxyhydroxides complexes. Therefore, it is expected that at high current, the extent of anodic dissolution increases (Faraday's law, Eq. 8), increasing oxyhydroxide cationic complexes and their subsequent roles in As removal (Kobya et al., 2015; Vasudevan et al., 2010). In this study, the effects of applied current (0.025–0.3 A) on As removal efficiency of EC reactor with an iron ball, scrap, and plate electrodes were investigated under three different groundwater resources (GW-1, GW-2, and GW-3).

4.1.1. As removal using Fe ball anodes

The effects of applied current (0.025–0.3 A) on As removal performance of EC process with iron ball electrodes were considered for different groundwater resources (GW-1, GW-2, and GW-3) and presented in Figure 2. At treatment of 538.8 μg/L of As containing GW-1 sample in cylindrical-shaped EC reactor with iron ball anodes, the highest As removal efficiencies were 99.7% ($C_{As,f}$: 2.3 μg L^{-1}), 99.8% ($C_{As,f}$: 1.1 μg L^{-1}), 99.9% ($C_{As,f}$: 0. μg L^{-1}), and >99.9% ($C_{As,f}$: 0.2 μg L^{-1}) for applied current of 0.025, 0.05, 0.1, and 0.3 A at operational time of 100 min, respectively (Figure 2a). These results could be explained by the increasing iron ball anode dissolution with the increasing applied current resulting in the generation of the larger size of flocs. Namely, when the applied current increases, simultaneously the water molecules on the cathode electrode surface are significantly reduced to generate H_2 and OH^- ions with the transport of Fe^{2+} and Fe^{3+} ions into solution via oxidation on the anode surface. Then, the metal hydroxides such as $Fe(OH)^{2+}$, $Fe(OH)^{+}_2$, $Fe(OH)_{3(s)}$, $Fe(OH)^{-}_4$, $Fe_2(OH)^{4+}_2$, and $Fe_3(OH)^{5+}_4$ are generated for iron ball electrodes (Moussa et al., 2017). These iron hydroxides are called “sweep flocs” and show a large surface area for adsorption of As in the GW sample. The OH^- ions in solution are attached to the *Fe oxyhydroxide* species. Subsequently, As species adsorption to these oxyhydroxide surfaces occurred by inner surface complexation. Moreover, the occurrence of water molecules between the oxyhydroxide surfaces and the As species assists other surface complexation (Mousazadeh et al., 2021).

These results showed that the enhanced applied current accelerated the As removal efficiency. For instance, the amount of Fe in GW-1 under an applied current of 0.3 A was almost 64.4 folds higher than that for the

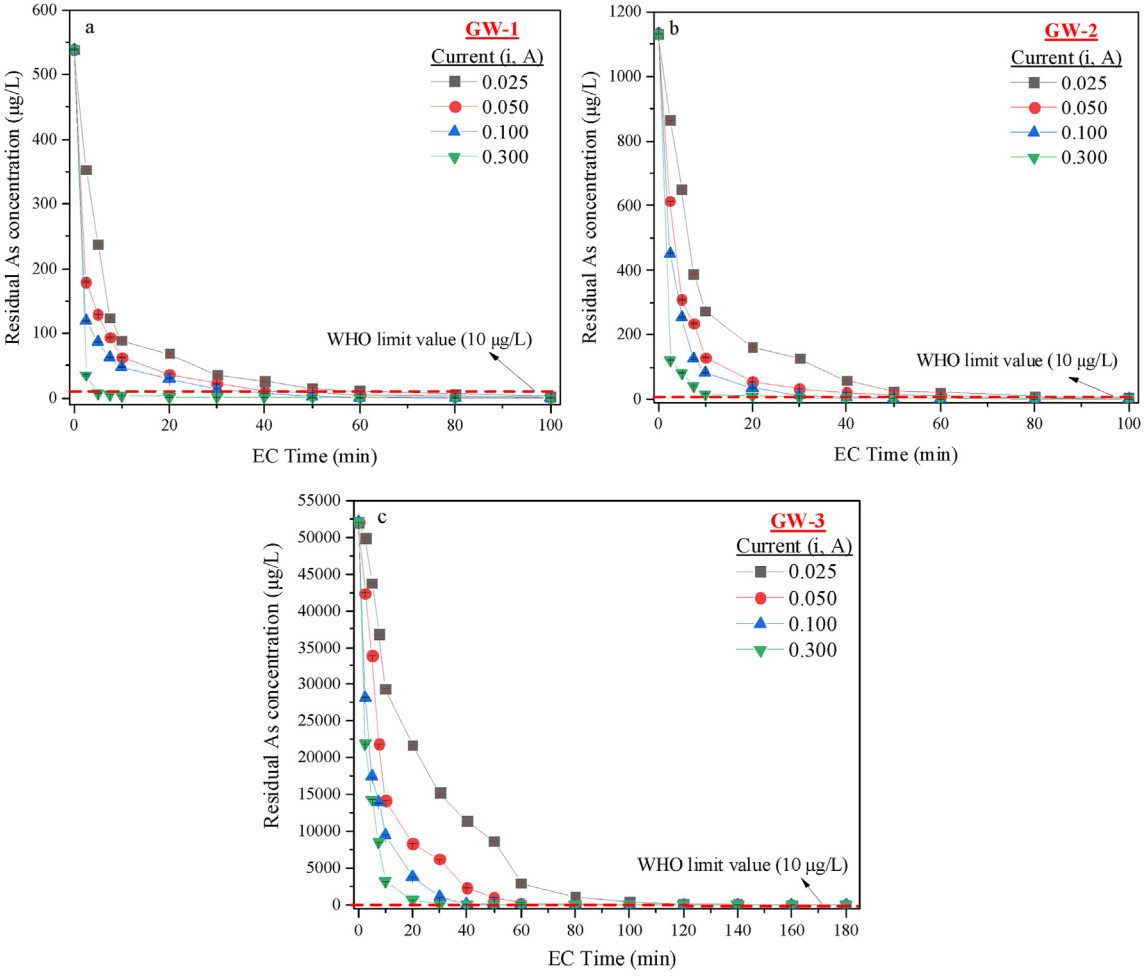

Figure 2. As removal from (a) GW-1, (b) GW-2, and (c) GW-3 at different currents using Fe ball anodes in cylindrical-shaped EC reactor.

applied current of 0.025 A at the end of the operating time of 100 min. Moreover, increasing the applied current decreased the operating time needed to achieve permissible As the concentration of 10 μg L^{-1} by WHO in drinking water. The effluent As concentrations were below the permissible level at the end of the operating time of 80, 50, 40, and 5 min for applied current of 0.025, 0.05, 0.1, and 0.3 A, respectively. For instance, at the end of the operating time of 80 min, the As removal efficiency was 98.8% under an applied current of 0.025 A, leading to an effluent As the concentration of 6.6 μg L^{-1}, which meets the WHO's guideline for 10 μg L^{-1} of As in drinking water. On the other hand, the effluent As concentration of 5 μg L^{-1} at an applied current of 0.3 A, which was below the allowable limit value of 10 μg L^{-1}, was reached after 5 min of operation time. As expected, the dissolution of Fe ball electrodes increased with increasing current density and the operating time needed to drop below the allowable As the concentration of 10 μg L^{-1} was significantly reduced (Kobya et al., 2015; Mendoza-Chávez et al., 2021). Furthermore, the As reduction was significantly quick up to the operating time of 10 min at all applied currents because of the occurrence of more arsenic particles in the GW-1 sample and then is reduced gradually as more hydrous ferric oxides formed enclosed structures with As over almost the whole interaction.

Effluent pH values in the GW-1 sample were also measured at the end of the operating time of 100 min for all experimental runs with different applied currents. Results showed that the pH of the GW-1 sample increased from 7.59 to 7.81 at an applied current of 0.025 A. This phenomenon can be explained with that the pH of the solution increases during the EC process because of the generation of H_2 gas and OH^- ions at the cathode electrode based on Eq. (3) (Thakur et al., 2019). In addition, the generated OH^- ions during the oxidation of Fe^{2+} to Fe^{3+} (Eq. 4) and the adsorption reaction between HFeO flocs and As (Eqs. (6) and (7)) also cause the pH increment at the end of the EC process. These results were in good agreement with literature studies (Zhu et al., 2007; Kobya et al., 2011; Sandoval et al., 2021).

However, the opposite or least meaningful trend was observed in other performed applied currents. This phenomenon most probably occurred due to the generation of water molecules at high current values (Lacasa et al., 2011). For instance, the effluent pH values of the GW-1 samples were found to be 7.32, 6.15, and 5.74 at the applied currents of 0.05, 0.1, and 0.3 A, respectively. The decrease in effluent pH can be also explained by the precipitation of iron hydroxide species and HFeO–As complexes with the utilization of OH^- ions, as presented in Eq. (5) (Maitlo et al., 2019). These results also confirmed that the reason for the significant decrease in the effluent pH values with the increasing current values is a result of more flock formation and their precipitation at high currents.

Similar As removal, pH variation, and Fe formation trends were observed in treatment of GW-2 and GW-3 samples under different applied currents with Fe ball anodes in a cylindrical-shaped EC reactor. For 1132.1 μg L^{-1} of As containing GW-2 sample treatment, the maximum As removal efficiencies were almost above 99.0% for all applied currents at an operational time of 100 min (Figure 2b). As expected, As removal performance of the EC process was enhanced with increasing applied current owing to the formation of considerable amount of iron hydroxide flock. For instance, As removal efficiency increased from 99.4% ($C_{As,f}$: 6.67 μg L^{-1}) to 99.8% ($C_{As,f}$: 1.85 μg L^{-1}) with increasing applied current from 0.025 to 0.3 A. The As effluent concentrations were achieved by the <10 μg L^{-1} of As limit value at operation times of 80, 40, and 30 min with the effluent concentration of 5.38, 8.76, and 6.1 μg L^{-1} under applied current of 0.05, 0.1, and 0.3 A, respectively. Moreover, the effluent pH values obtained in the treatment of the GW-2 sample showed the same trend as the results of the treatment of the GW-1 sample. A significant pH variation was observed at the current density of 0.3 A with a decrease from 8.11 to 7.22 most probably due to the high Fe formation (0.56595 g Fe) and HFeO–As complex precipitation. On the other hand, a slight pH variation was observed at the applied current of 0.025 A with a decrease from 8.11 to 7.7 because of the low Fe generation (0.04829 g Fe). At 52,000 μg L^{-1} of As containing GW-3 sample treatment, the maximum As removal efficiencies were >99.9% for all applied currents at an operational time of 180 min (Figure 2c). Similar to other GW treatment experiments, the operational time required to reduce the As concentration below 10 μg L^{-1} was decreased with increasing applied current owing to enhancing dissolution rate of Fe ball electrodes with high iron hydroxide-arsenic complex formation at high currents. As expected, the shortest time required for the As concentration to decrease below 10 μg L^{-1} was found as 60 min at the applied current of 0.3 A and the effluent As amount was measured as 4.12 μg L^{-1}. On the other hand, the operational time required to reduce the As concentration below 10 μg L^{-1} was found to be 140 min for both applied current of 0.05 and 0.1 A, while it was 180 min for 0.025 A applied current. This phenomenon can be explained by the accelerated anodic dissolution and Fe formation in GW samples owing to high currents. The amount of Fe was found as 0.08319 g for applied current of 0.025 A, while it was 1.00834 g for an applied current of 0.3 A at an operational time of 180 min. Furthermore, the initial pH value was increased by almost 1.02 folds at the end of the EC experiments under all applied currents due to the formation of OH^- ions. The effluent pH value was in the range of 9.96–6.99.

Overall, these results showed that the EC process with Fe ball anodes significantly removed As from different GW samples. Moreover, the performance of the EC process increased with increasing applied current. However, the time required to decrease As concentration below the 10 μg L^{-1} was highest in the GW-3 sample, while it was lowest in the GW-1 sample. This is because a higher amount of As were measured in the GW-3 sample, while relatively few values were observed in GW-1 and GW-2 samples.

4.1.2. As removal using Fe scrap anodes

Treatment of GW-1, GW-2, and GW-3 samples was also performed using iron scrap electrodes at different applied currents. The effects of applied current on EC process performance are presented in Figure 3. At an operational time of 100 min, the maximum As removal efficiencies were >99.9% for all applied current values in the treatment of the GW-1 sample (Figure 3a). To achieve permissible As limit value of 10 μg L^{-1}, the minimum operational times were found as 30, 20, 10, and 7.5 min for applied current of 0.025, 0.05, 0.1, and 0.3 A with As removal efficiency of 98.5% ($C_{As,f}$: 8.1 μg L^{-1}), 98.9% ($C_{As,f}$: 6.2 μg L^{-1}), 98.3% ($C_{As,f}$: 9.35 μg L^{-1}), and 98.9% ($C_{As,f}$: 6.1 μg L^{-1}), respectively. These results revealed that the time to achieve the permissible As limit value significantly decreased as the current was increased from 0.025 to 0.3 A. Namely, the quantity of anode electrode dissolution in the EC reactor is exactly proportional to the amount of electricity transferred the in solution, according to Faraday's law (Eq. 8). Hence, since more charge is transmitted through the system, more coagulant dose (Fe^{3+}) and gas bubble formation (H_2 and O_2) develop, which promotes mixing within the EC reactor. In other words, when charge loading rises, the proportion of electrochemically dissolving Fe scrap electrode increases as well, resulting in increased As removal efficiency. Finally, more EC time boosts the formation of Fe^{2+}, Fe^{3+}, and OH^- ions, improving contaminant removal through the formation of iron hydroxide flocs (Kobya et al., 2021). For instance, the Fe formation increased from 0.05790 g to 0.68328 g with increasing applied current from 0.025 to 0.3 A at 100 min. Moreover, the effluent pH values were measured at the end of the experimental runs. While the effluent pH values increased at 0.025 and 0.05 A current density, the effluent pH values decreased at 0.1 A and 0.3 A. The reason for this situation can be explained by the fact that while the ferric hydroxide complexes formed at high current values are more, fewer complexes are formed at low current densities and OH^- ions remain free in the solution.

In the treatment of the GW-2 sample, attaining As removal efficiency of 99.9% (As a reduction from 1132.1 to almost 0.1 μg L^{-1}) required an operational time of 100 min under all the applied currents (Figure 3b). The time to achieve <10 μg L^{-1} As concentration remarkably reduced as

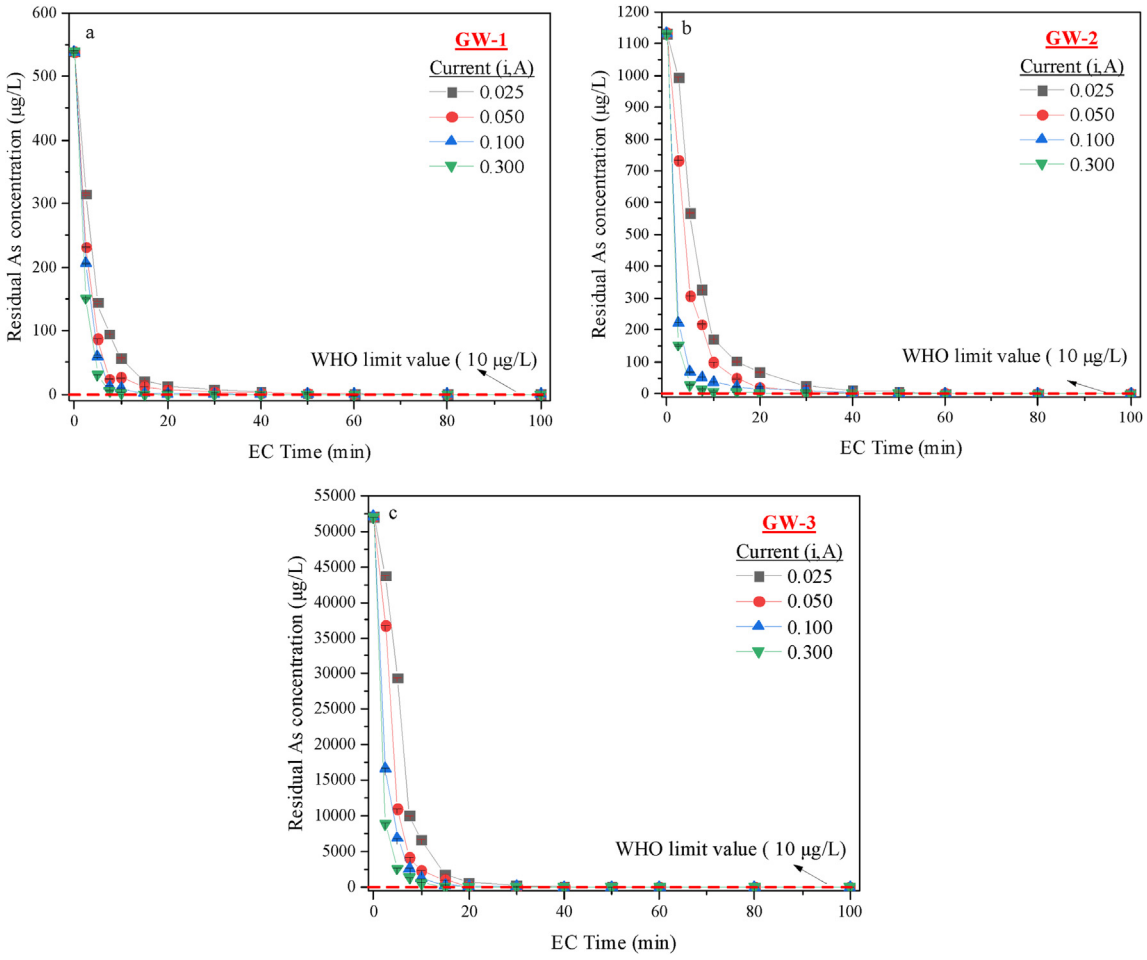

Figure 3. As removal from (a) GW-1, (b) GW-2, and (c) GW-3 at different currents using Fe scrap anodes in cylindrical-shaped EC reactor.

the applied current was raised from 0.025 to 0.3 A. For instance, residual As concentration at an operational time of 30 min was found to be 25.8, 5.58, 9.86, and 1.5 µg L^{-1} for 0.025, 0.05, 0.1, and 0.3 A, respectively. In view of the applied currents, 0.3 A emerges to be the optimum current. Namely, As concentration dropped below 10 µg L^{-1} in 10 min at 0.3 A and 30 min at 0.05 and 0.1 A. Moreover, the pH variation for 0.3 A was higher than for 0.025 A due to the formation of a significant amount of iron hydroxide complexes. The initial pH decreased from 8.11 to 8.04 at 0.025 A, while the effluent pH value was 7.62 at 0.3 A.

The results obtained in the GW-3 sample treatment were consistent with the results obtained in GW-1 and GW-2 treatments. The As removal efficiency increased with increment in applied current. The highest As removal efficiencies were >99.9% with effluent As concentrations of 3.75, 2.65, 1.2, and 0.13 µg L^{-1} for applied current of 0.025, 0.05, 0.1, and 0.3 A at operational time of 100 min, respectively (Figure 3c). As concentration dropped below 10 µg L^{-1} in 80 min at 0.025 and 0.05 A, 60 min at 0.1 A, and 40 min at 0.3 A. However, the time required for effective As removal in the treatment of GW-3 sample has increased significantly, since the inlet As concentration is higher than in other GW samples. For instance, while the time required to reduce the As concentration below 10 µg L^{-1} at a current of 0.3 A was 7.5 min in the GW-1 treatment, this time was found to be 40 min in the GW-3 treatment. A similar trend was observed at all applied currents. As expected, with increasing As concentration, the operational time also increased. Namely, when the initial As concentration was higher, more iron hydroxide was needed to reduce the dissolved As concentrations. Consequently, As removal was limited by the formation rate of iron hydroxide species in the treatment of the GW-3 sample.

4.1.3. As removal using Fe plate anodes

The As removal performance of rectangular EC reactor with Fe plate electrodes from GW samples was investigated under different applied currents. In the treatment of the GW-1 sample, it can be clearly seen from Figure 4a that As removal was greater than 98.5% and the effluent As concentrations obtained were less than 10 µg L^{-1} after 10 min operational time was passed at 0.1 and 0.3 A. On the other hand, the effluent As concentration was dropped below 10 µg L^{-1} after an operational time of 30 and 40 min for 0.05 and 0.025 A, respectively. It can be also concluded from Figure 4 that a sharp decrease in As concentration just at the beginning of the experiments for all current densities and GW samples occurred. In general, the removal of the As is fast at the start of the treatment, then diminished over the time of practically the whole process. The species of As are so much more plentiful during the beginning of the process, that the produced iron hydroxides due to anode corrosion can easily form complexes with As at that time, resulting in fast As reduction (Amrose et al., 2013; Ucar et al., 2013). Nevertheless, as the experiment continues, the aqueous solution As concentration decreases while the concentration of hydrous ferric oxides rises, resulting in an excess of hydrous ferric oxides at the end of the operation. As a result, the curves are virtually identical at the end of the experiment. Moreover, the amount of Fe generated during the EC process increased linearly with operational time. For GW-1 treatment at the applied current of 0.1 A, 0.5321 g Fe was produced over the 100 min experimental duration, while it was 0.0532 g Fe at the end of the operational time of 10 min. A similar trend observed at other current values.

Similarly, by increasing the applied current from 0.025 to 0.3 A the As removal efficiency is further enhanced in the treatment of the GW-2

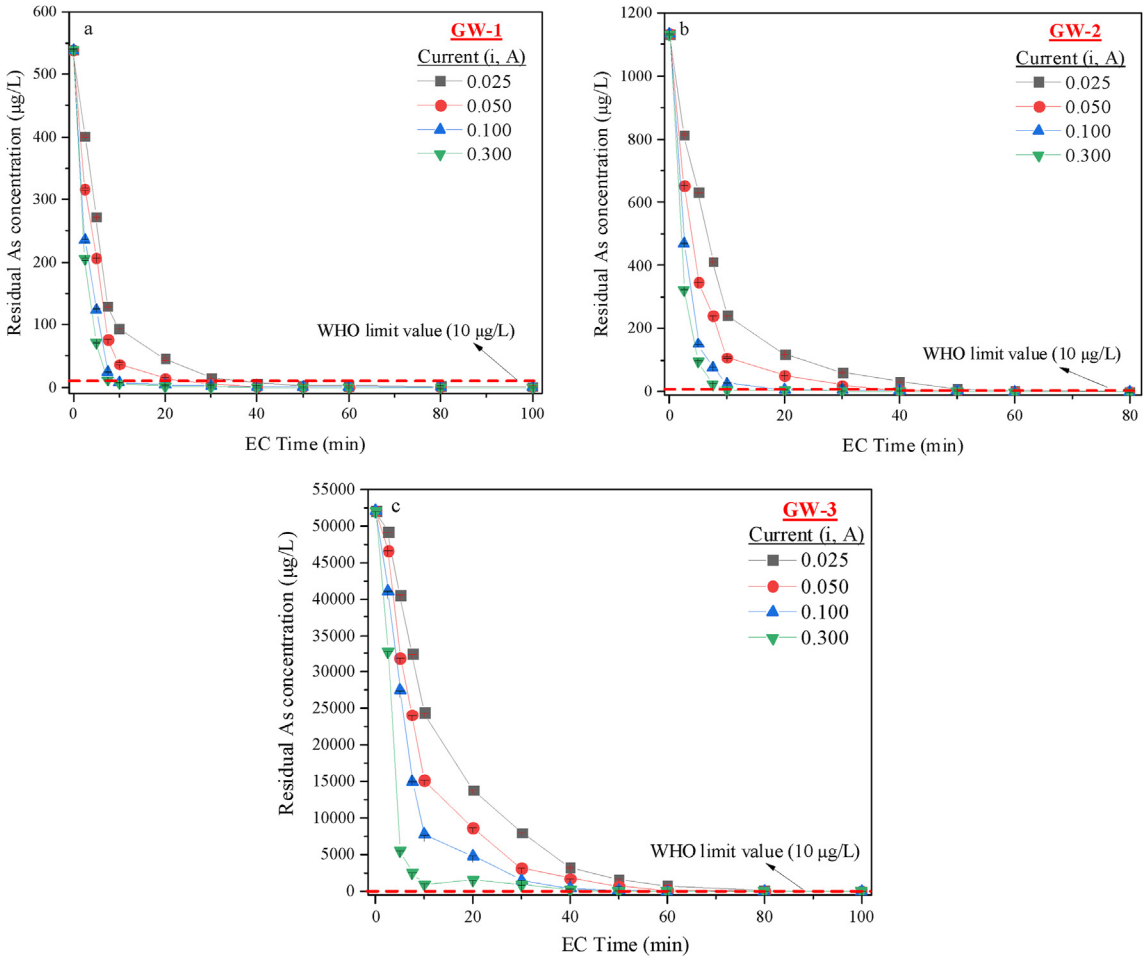

Figure 4. As removal from (a) GW-1, (b) GW-2, and (c) GW-3 at different currents using Fe plate anodes in rectangular EC reactor.

sample (Figure 4b). The maximum As removal efficiencies were found to be above >99.9% under all applied currents at an operational time of 80 min. Moreover, these results showed that the dissolution of Fe plate electrodes was improved with increasing current. The highest Fe production was 0.4324 g for 0.3 A, while it was 0.0264 g for 0.025 A at the end of the experimental runs. As expected, the EC process decreased the initial As the concentration of 1132.1 µg L^{-1} to less than the WHO limit value of 10 µg L^{-1} at the applied current of 0.3 A and operational time of 10 min. On the other hand, the minimum operating time required to achieve the WHO limit value was found to be 20, 40, and 50 min with effluent As concentrations of 7.64, 4.33, and 9.44 µg/L for 0.1, 0.05, and 0.025 A, respectively. On the other hand, when the currents were 0.025 and 0.05 A in the case of GW-3 sample treatment, the operating time and effluent As concentrations were 100 min and 11.42 µg L^{-1} (99.98%) for 0.025 A and 100 min and 7.65 µg L^{-1} (99.99%) for 0.05 A, and As was effectively removed in 60 min with effluent As concentration of 1.65 µg L^{-1} as the current increased to 0.3 A (Figure 4c). In a conclusion, these results showed that the As removal from the GW-3 sample took more time to get below the permissible value for As the GW had a higher initial As concentration. This finding might be explained by the fact that further ferrous hydroxides/oxyhydroxides were required to decrease the dissolved As when the starting concentrations were higher.

Overall, considering all GWs treatment in different currents, the highest operational time is obtained for ball anodes and the lowest time for scrap anodes. Fe scrap anodes were more affected than Fe plate and ball anodes due to the decreasing the operational time to less than half its value, which also significantly affects the operation and maintenance cost of the EC process. The dissolution of anodes presented a different performance for the shape of the electrode based on Faraday's Law. Namely, in the treatment of GW-3 sample at the applied current of 0.3 A, the As removal efficiency (>99.9%) using Fe scrap anodes was quicker almost 1.7 and 2.5 folds than that for Fe ball and plate anodes because of the amount of dissolved Fe in solution. This phenomenon could be explained by the that Fe scrap anodes have a larger electrode contact surface area than the plate and ball anodes, therefore providing a high contact area between the anodes and As species in the EC reactor, leading to an overall increase in EC process As removal efficiency (Kobya et al., 2021; Elazzouzi et al., 2021). When the Fe scrap anodes were performed for GW-1 sample treatment, effluent As concentrations decreased to <10 µg L^{-1} after an operational time of 7.5–30 min. On the other hand, higher operational times as 10–40 min and 5–80 min were needed to reach the same effluent As concentration and removal performance in the case of Fe plate and ball anodes, respectively. For instance, the As removal efficiency of >99.9% in GW-3 sample at 0.3 A was achieved using Fe scrap anodes within the operational time of 40 min, while EC reactor operated with Fe plate and ball anode needed a significantly longer time (60–100 min) under same operating conditions. These results are lower than the reported values in the literature. For instance, the treatment of 80.2 µg L^{-1} of As containing real GW was performed using the EC process with iron electrodes and the minimum operating time of 30 min with As removal efficiency of 85.2% was achieved to drop As concentration below 10 µg L^{-1} at the applied current of 0.2 A (Mendoza-Chávez et al., 2021). Consequently, our results revealed that the As removal performance of the EC reactor was significantly effective when Fe scraps were used as an anode material, considering As removal efficiency, effluent As concentration, dissolved Fe production rate, and operational time.

4.2. Evaluation of operating cost

In this paper, the As removal efficiency of the EC process was evaluated from a technical point of view, but the overall performance of the EC process needs to be evaluated in terms of operating costs considering energy and electrode consumption and sludge disposal cost. Electrode and electrical energy consumptions are very important economical parameters in the EC process (Kobya et al., 2015). Therefore, the energy (C_{energy}) and electrode ($C_{electrode}$) consumption costs are a major part of the operating cost in the EC process. The electrode consumption was calculated using Eq. (8):

$$C_{electrode} = \frac{i \times t_{EC} \times M_w}{z \times F \times v} \quad \text{Eq. 8}$$

where $C_{electrode}$ (kg Fe electrode per m^3 treated GW sample) is the theoretical amount of Fe ions produced by applied current i (A) passed for a duration of operating time t_{EC} (s), z is the number of electrons involved in the oxidation/reduction reaction; for Fe ($z = 2$). M_w is the atomic weight of iron anode material ($M_w = 55.85$ g mol^{-1}), F is the Faraday's constant (96485 $C\ mol^{-1}$), and v is the volume (m^3) of the GW sample in the EC reactor (0.94 mL). The energy consumption was also calculated using Eq. (9):

$$C_{energy}\left(kWh \Big/ m^3\right) = \frac{i \times t_{EC} \times U}{v} \quad \text{Eq. 9}$$

where i is applied current (A), U is cell voltage (V), t_{EC} is EC time (hour for energy consumption or sec for electrode consumption), and v is the volume (m^3) of the GW sample in the EC reactor. $C_{electrode}$ (kg m^{-3}) is the kg amount of electrode consumed in removing As from one cubic meter of GW.

Moreover, the total operating costs (OC) for removing As from GWs were calculated by taking into consideration of the energy (C_{energy}) and electrode ($C_{electrode}$) consumptions, and sewage sludge (C_{sludge}) disposal cost by following Eq. (10):

$$OC = \alpha C_{energy} + \beta C_{electrode} + \gamma\ C_{sludge} \quad \text{Eq. 10}$$

where OC ($/$m^3$) is the number of dollars required to treat one cubic meter of groundwater, C_{energy} (kWh/m^3) is kilowatt-hours consumed per cubic meter of treated groundwater, $C_{electrode}$ (kg m^{-3}) is the kg amount of electrode consumed in removing As from one cubic meter of groundwater, and C_{sludge} (kg m^{-3}) is the cost of disposal of sludge amount of one cubic meter of treated water. For Turkey in June 2021, the costs of unit energy (α), electrode (β), and sludge disposal (γ) is 0.120 \$ kWh^{-1}, 5.1 \$ kg^{-1}, and 0.152 \$ kg^{-1}, respectively. In addition, the costs of iron plate, ball, and scrap anodes are 0.952, 4.50, and 0.20 \$ kg^{-1}, respectively.

Operating costs, energy and electrode consumptions were calculated for conditions where effluent As concentration dropped below the 10 μg L^{-1} in all GWs using different anodes and outputs are reported in Table 2. Results revealed that the consumption of energy and electrode, thus the operating cost, increased with increasing currents in the treatment of all GWs. In treatment of GW-1, the values of the energy and electrode consumption at 0.025–0.1 A increased from 0.0468 to 0.2787 kW h m^{-3} and 0.0424–0.0750 kg m^{-3} for Fe ball anodes, from 0.085 to 0.0263 kW h m^{-3} and 0.0192–0.0199 kg m^{-3} for Fe plate anodes, and from 0.0073 to 0.0234 kW h m^{-3} and 0.0185–0.0212 kg m^{-3} for Fe scrap anodes. As expected, the minimum electrode and energy consumption with low operating cost was observed using Fe scrap anodes owing to their significant surface area resulting in the high amount of Fe dissolution. In the case of GW-1 treatment, the operating costs at 0.025–0.3 A were in the range of 0.2141–0.4208 \$ m^{-3} for Fe ball anodes, 0.0257–0.1336 \$ m^{-3} for Fe plate anodes, and 0.0219–0.1079 \$ m^{-3} for Fe scrap anodes. When the operating costs of the anodes were compared, it was found that the highest operating cost of 0.4208 \$ m^{-3} was calculated for Fe ball anodes at 0.3 A, while the lowest operating cost was 0.0219 \$ m^{-3} for Fe scrap anodes at 0.025 A. These results showed that 0.025 A current is effective in order to reduce the As concentration below 10 μg L^{-1} and to provide minimum cost. However, when evaluating the EC performance, the real scale applicability, cost and treatment time should be considered simultaneously. Although the lowest cost was found at a low current density, the treatment time was found to be 30 min. Therefore, it can be proposed that the optimum operating conditions for reduction of As concentration below 10 μg L^{-1} in GW-1 sample was a current of 0.1 A and an operational time of 10 min with the operating cost of 0.0336 \$ m^{-3}. Our results were in good agreement with literature studies. The operational cost of the Fe ball, scrap, and plate anodes was mostly lower than that for the literature studies with Al and Fe anodes. For instance, Valentín-Reyes et al. (2022) investigated the treatment of As from groundwater using a continuous flow EC process with iron plate anodes. The maximum As removal efficiency was reported to be <10 μg L^{-1} (74%) at the current density of 6 mA cm^{-2} and flow rate of 2.3 cm s^{-1} with an operational cost of 0.178 USD m^{-3}. In a separate study for As removal from natural groundwater with EC process using Al plate anodes, the operational cost was found to be 0.48 USD m^{-3} (Gutiérrez et al., 2022).

Table 2. Operating cost, energy, and electrode consumption for As removal using different anodes.

i (A)	GW-1			GW-2			GW-3		
	C_{energy} (kWh m^{-3})	$C_{electrode}$ (kg m^{-3})	OC (\$ m^{-3})	C_{energy} (kWh m^{-3})	$C_{electrode}$ (kg m^{-3})	OC (\$ m^{-3})	C_{energy} (kWh m^{-3})	$C_{electrode}$ (kg m^{-3})	OC (\$ m^{-3})
Fe ball anodes									
0.025	0.0468	0.0424	0.2141	0.1228	0.0483	0.2330	0.1412	0.0832	0.4056
0.050	0.0931	0.0476	0.2462	0.4624	0.0755	0.3954	0.2606	0.1302	0.6760
0.100	0.2787	0.0750	0.3940	0.6511	0.0754	0.4176	0.6330	0.2676	1.3657
0.300	0.1883	0.0283	0.4208	1.7585	0.1698	0.9991	1.2160	0.3361	1.7728
Fe plate anodes									
0.025	0.0085	0.0192	0.0257	0.0335	0.0245	0.0223	0.0235	0.0467	0.0813
0.050	0.0245	0.0281	0.0335	0.0798	0.0374	0.0531	0.0621	0.0946	0.1349
0.100	0.0263	0.0199	0.0477	0.1043	0.0391	0.0616	0.1248	0.1537	0.1949
0.300	0.1511	0.0566	0.1336	0.4367	0.0575	0.1302	0.4660	0.3448	0.4239
Fe scrap anodes									
0.025	0.0073	0.0185	0.0219	0.0211	0.0340	0.0262	0.0192	0.0469	0.0815
0.050	0.0134	0.0197	0.0303	0.0825	0.0386	0.0649	0.0575	0.0885	0.1118
0.100	0.0234	0.0212	0.0336	0.1649	0.0678	0.0767	0.0787	0.1247	0.1323
0.300	0.1133	0.0545	0.1079	0.4223	0.0845	0.1571	0.2404	0.2660	0.1719

A similar trend was observed in the treatment of the GW-2 sample. The highest energy consumption was found using Fe ball anode electrodes with a value of 1.7585 kW h m^{-3} at 0.300 A, while the minimum energy consumption was found as 0.0211 kW h m^{-3} with scrap anodes at 0.025 A. Electrode consumption was the lowest with plate anodes at 0.025 A with a value of 0.0245 kg m^{-3}, while it showed the highest value at 0.300 A for ball electrodes with a value of 0.1698 kg m^{-3}. The minimum operating cost was calculated as 0.0262 $ m^{-3} with scrap electrodes at 0.025 A, and the highest value at 0.9991 $ m^{-3} with ball anodes at 0.300 A. For treatment of the GW-3 sample, the highest energy consumption at 0.300 A with ball electrodes with a value of 1.216 kW h m^{-3}, scrap Fe anodes had a minimum value of 0.0192 kW h m^{-3} at 0.025 A. While the highest electrode consumption was 0.3448 kg $m^{-3}$with plate electrodes at 0.300 A, the lowest was calculated as 0.0467 kg m^{-3} at 0.025 A with plate electrodes. The operating cost was the highest with ball anodes at 0.300 A with a value of 1.773 $ m^{-3}, while at 0.025 A with plate anodes, 0.0813 $ m^{-3} had the lowest value.

Moreover, since the As amounts of the treated GWs were different, it has been observed that the operating cost increased with the increasing As concentration due to the increasing operating time to reduce As below 10 μg L^{-1}, as expected. For example, the operating cost for the treatment of GW-1 sample was 0.4208 $ m^{-3} at current of 0.3 A using ball anodes, while it was calculated to be 1.7728 $ m^{-3} in treatment of GW-3 sample. Similar trends were observed for the other anodes. These results showed that the scrap anodes were found to be the most suitable material considering minimum operational time and operating cost to reduce As below the permissible limit value. Moreover, the results also showed that the residual Fe concentration in treated water was satisfied the WHO standard (3.0 mg L^{-1}) (WHO, 2011). Consequently, there is no need for further post-treatment to assure the GW quality when we consider the residual As and Fe concentration in treated water. On the other hand, we propose using sources of renewable energy such as solar, hydroelectric generators, and wind, based on the practicality of the location, if the EC process is planned to be built into a large-scale treatment facility to address the water requirements of contaminated areas. With this approach, the operational expenses including energy consumption of DC power supply and air compressor will be drastically reduced. The OC reported in this study are relatively low and much more encouraging than just those found in research through Sorg et al. (2015) that examined the expense of removing As in groundwater in the USA utilizing various removal technologies, including adsorption, coagulation-filtration, treatment with iron, ion exchange resins, and reverse osmosis to decrease As to <10 μg L^{-1} Sorg et al. (2015) found maintenance and OC for adsorption, ion exchange resin, and combined iron treatment with coagulation-filtration to be 6.66, 1.85, and 1.06 US $ m^{-3}, respectively. It is clear that variations in the experimental studies are what cause the OC variances. Therefore, the utilization of Fe anodes demonstrates to be a costly treatment method for As removal in groundwater.

4.3. Arsenic removal capacity

The As removal capacity per quantity of iron dissolved electrochemically (q_e, μgAs $mgFe^{-1}$ or qe, μgAs C^{-1}) was determined from Eqs. (11) and (12) and the results are presented in **Figure SM1-SM3**.

$$q_e\,(\mu gAs\,/\,mgFe) = \frac{(C_o - C_f)}{C_{electrode}} \qquad \text{Eq. 11}$$

$$q_e\,(\mu gAs\,/\,C) = \frac{(C_o - C_f)}{q} \qquad \text{Eq. 12}$$

where C_o is initial As concentrations (μg L^{-1}), C_f is the As concentrations at any operating time (μg L^{-1}), and $C_{electrode}$ (kg m^{-3}) is the kg amount of electrode consumed in removing As from one cubic meter of GW. The operating cost per m^3 of EC treated-water increases with charge loading due to the increasing energy cost. Therefore, the optimization of charge loading is important considering EC process necessities and water physicochemical quality. The charge loading was calculated using current and operating time with Eq. (13) (Omwene et al., 2019):

$$q(C) = i \times t_{EC} \times CF \qquad \text{Eq. 13}$$

where q is the charge loading (Coulomb), i is applied current (A), CF is conversion factor (60), and t_{EC} is operational time (s). High charge loading values cause a significant amount of metal hydroxide flock generation and these excessive generations affect the residual iron concentration, causing the formation of iron higher than the required dosage (Mohora et al., 2018).

The As removal capacities (q_e), charge loading (q), and dissolved iron amounts (m_{Fe}) in GWs are given in Table 3 for different anode materials. The effluent As concentration was decreased with increment in charge loading for all anodes in GWs. In the case of GW-3 treatment, the charge loading values needed to reach As concentrations of <10 μg L^{-1} were 270, 420, 840, and 1080 C at currents of 0.025, 0.05, 0.1, and 0.3 A, respectively, for Fe ball anodes. On the other hand, the charge loading values were in the range of 150–1080 and 120–720 C for Fe plate and scrap anodes at currents of 0.025–0.3 A, respectively. These results revealed that the charge loading values for Fe scrap anodes were lower than that for plate and ball anodes since the needed operational time to drop As concentration below 10 μg L^{-1} using Fe scrap anodes was lower than that the plate and ball anodes. These phenomena are also confirmed by the charge loading values calculated for different GWs. Namely, the charge loading values were increased with increasing As concentration in GW samples due to the high operational time. For instance, the charge loading values were 135, 180, and 729 C in the treatment of GW-1, GW-2, and GW-3 samples, respectively, using Fe scrap anodes at 0.3 A. As the operational time and As concentration increased, the amount of iron and the needed charge loading also increased. A similar trend was observed for the other anode materials and applied currents. Our results showed good agreement with the reported values in literature (Omwene and Kobya, 2018; Dutta et al., 2021).

Moreover, the As adsorption capacities of all anode materials for GWs were calculated. For current of 0.025–0.3 A, the As adsorption capacities using Fe ball anodes varied from 11.80 to 17.62 μgAs $mgFe^{-1}$ (4.17–5.55 μgAs C^{-1}) for GW-1, 21.9 to 6.23 μgAs $mgFe^{-1}$ (7.05–1.96 μgAs C^{-1}) for GW-2, and 587.49 to 145.42 μgAs $mgFe^{-1}$ (181.01–45.26 μgAs C^{-1}) for GW-3. As expected, the adsorption capacity increased with increasing As concentration in GWs. A similar trend was observed using Fe scrap and plate anodes. In general, all anodes presented a decreasing trend in adsorption capacity of As with increasing current and operational time (except for GW-1 sample treatment using Fe ball electrodes). In this study, the adsorption capacity was determined as the removed amount of As per the amount of dissociated iron using Eq. (11). The As reduction is initially high, then slowly decreases to a stable rate, this trend most probably occurred due to the decrease in the amount of As accessible for precipitation, co-precipitation, ligand exchange and decrease in As adsorption capacity of iron hydroxides at diminished As concentrations (**Figure SM1-SM3**). The amount of dissolved iron was also measured to understand the effect of current on the amount of iron in GW samples. As expected, the dissolved iron amount was increased with an increasing current values for all GW samples (except for GW-1 sample treatment using Fe ball electrodes). For instance, in GW-1 treatment using Fe scrap anodes, the amount of iron increased from 17.37 to 51.25 mg with increasing current from 0.025 to 0.3 A. Furthermore, results proved that the dissolved iron amount increased with increasing operational time. Namely, the amount of iron was found to be 51.25, 84.46, and 249.99 mg in the treatment of GW-1, GW-2, and GW-3 samples using Fe scrap anodes at 0.3 A and operational times of 7.5, 10, and 40 min, respectively. A similar trend was observed for other anode materials. For Fe plate electrodes, the dissolved iron amount was in the range of 53.21–324.07 mg at 0.3 A, while it was in the range of 28.34–336.11 mg for Fe ball anodes.

Table 3. As removal capacity and iron production of EC process using different anodes.

i (A)	GW-1				GW-2				GW-3			
	m_{Fe} (mg Fe)	q (C)	q_e (μgAs $mgFe^{-1}$)	(μgAs C^{-1})	m_{Fe} (mg Fe)	q (C)	q_e (μgAs $mgFe^{-1}$)	(μgAs C^{-1})	m_{Fe} (mg Fe)	q (C)	q_e (μgAs $mgFe^{-1}$)	(μgAs C^{-1})
Fe ball anodes												
0.025	42.38	120	11.80	4.17	48.30	150	21.90	7.05	83.19	270	587.49	181.01
0.050	47.56	150	10.49	3.32	75.49	240	14.03	4.41	130.23	420	375.29	116.37
0.100	75.02	240	6.66	2.08	70.84	240	14.91	4.40	267.58	840	182.65	58.18
0.300	28.34	90	17.62	5.55	169.79	540	6.23	1.96	336.11	1080	145.42	45.26
Fe plate anodes												
0.025	18.08	60	27.66	8.34	23.06	75	45.75	14.07	43.90	150	1113.23	325.80
0.050	26.43	90	18.98	5.57	35.20	120	30.12	8.83	88.90	300	549.75	162.91
0.100	18.67	60	26.74	8.32	36.72	120	28.78	8.81	144.48	480	338.29	101.82
0.300	53.21	180	9.40	2.78	54.05	180	19.58	5.88	324.07	1080	150.82	45.26
Fe scrap anodes												
0.025	17.37	45	28.72	11.09	34.01	75	31.11	14.11	44.08	120	1108.77	407.28
0.050	18.48	60	27.09	8.34	33.60	90	31.51	11.77	83.20	240	587.41	203.63
0.100	19.94	60	24.96	8.29	67.80	180	15.56	5.86	117.25	360	416.84	135.76
0.300	51.25	135	9.77	3.71	84.46	180	12.53	5.88	249.99	720	195.50	67.88

Overall, these results showed that the lowest As adsorption capacity was observed for Fe ball anodes. On the other hand, no significant difference was observed between the adsorption capacities obtained for plate and scrap anodes. Although the adsorption capacity obtained for Fe plate anodes is higher than scrap anodes, scrap anodes emerge as a more effective material than plate anodes thanks to their high removal efficiency, low operating cost and operational time, and high surface area.

5. Conclusion

All anode materials decreased the effluent As concentration to the WHO standard. However, the Fe scrap anodes performed better As removal when compared with Fe ball and plate anodes. For Fe scrap electrodes to reach an effluent As concentration of 10 μg L^{-1}, optimum conditions were obtained as the operational time of 7.5, 10, and 40 min with a removal efficiency of 98.9, 99.4, and >99.9% in the treatment of GW-1, GW-2, and GW-3, respectively, at the current of 0.3 A. On the other hand, under the same operational conditions, the operational time of the EC process for Fe plate and ball anodes was higher than that for scrap anodes due to the high As concentration in GW-3. Moreover, at 0.025 A, minimum operating costs for the GW-1 and GW-2 and GW-3 samples were 0.2141, 0.2230 and 0.4056 $ m^{-3} for Fe ball anodes; 0.0257, 0.0323 and 0.0813 $ m^{-3} for Fe plate anodes, and 0.0219, 0.0262 and 0.0815 $ m^{-3} for Fe scrap anodes, respectively. These results showed that Fe scrap anodes were 5 folds more economical than Fe ball anodes at 0.025 A in the treatment of GW-1, while there was no significant difference compared with Fe scrap and plate anodes. On the other hand, the scrap anodes were almost 10.3 and 1.5 folds more economical than ball and plate anodes at 0.1 A in treatment of GW-3. Overall, this study proved that the EC process with cost-effective Fe scraps anodes was promising and effective in GW treatment with its significant potential in field application, especially high As containing GWs, considering minimum operating cost and operational time.

Declarations

Author contribution statement

Mehmet Kobya: Contributed reagents, materials, analysis tools or data; Conceived and designed the experiments.

Mustafa Dolaz: Wrote the paper; Contributed reagents, materials, analysis tools or data.

Burcu Özaydın-Şenol: Performed the experiments; Analyzed and interpreted the data.

Aysegul Yagmur Goren: Wrote the paper; Analyzed and interpreted the data.

Funding statement

This research did not receive any specific grant from funding agencies in the public, commercial, or not-for-profit sectors.

Data availability statement

Data will be made available on request.

Declaration of interests statement

The authors declare no conflict of interest.

Additional information

Supplementary content related to this article has been published online at https://doi.org/10.1016/j.heliyon.2022.e10489.

References

Alcacio, R., Nava, J.L., Carreno, G., Elorza, E., Martinez, F., 2014. Removal of arsenic from deep well by electrocoagulation in a continuous filter press reactor. Water Sci. Technol. Water Supply 14, 189–195.

Amrose, S., Gadgil, A., Srinivasan, V., Kowolik, K., Muller, M., Huang, J., Kostecki, R., 2013. Arsenic removal from groundwater using iron electrocoagulation: effect of charge dosage rate. J. Environ. Sci. Health A. 48, 1019–1030.

APHA (American Public Health Association), 1998. Standard Methods for the Examination of Water and Wastewater, 20th end. Washington DC, USA.

Banerji, T., Chaudhari, S., 2016. Arsenic removal from drinking water by electrocoagulation using iron electrodes- an understanding of the process parameters. J. Environ. Chem. Eng. 4, 3990–4000.

Bordoloi, S., Nath, S.K., Gogoi, S., Dutta, R.K., 2013. Arsenic and iron removal from groundwater by oxidation–coagulation at optimized pH: laboratory and field studies. J. Hazard Mater. 260, 618–626.

Choong, T.S.Y., Chuah, T.G., Robiah, Y., Koay, F.L.G., Azni, I., 2007. Arsenic toxicity, health hazards and removal techniques from water: an overview. Desalination 217, 139–166.

Çöl, M., Çöl, C., 2004. Arsenic concentrations in the surface, well, and drinking waters of the Hisarcik, Turkey, Area. Hum. Ecol. Risk Assess. 10, 461–465.

Çolak, M., Gemici, Ü., Tarcan, G., 2003. The effects of colemanite deposition the arsenic concentrations of soil and groundwater in Igdeköy-Emet, Kutahya, Turkey. Water Air Soil Pollut. 149, 127–143.

Dogan, M., Dogan, A.U., 2007. Arsenic mineralization, source, distribution, and abundance in the Kutahya region of the western Anatolia, Turkey. Environ. Geochem. Health 29, 119–129.

Dutta, N., Haldar, A., Gupta, A., 2021. Electrocoagulation for arsenic removal: field trials in rural West Bengal. Arch. Environ. Contam. Toxicol. 80, 248–258.

Elazzouzi, M., Haboubi, K., Elyoubi, M.S., El Kasmi, A., 2021. Development of a novel electrocoagulation anode for real urban wastewater treatment: experimental and modeling study to optimize operative conditions. Arab. J. Chem. 14, 102912.

Garcia-Lara, A.M., Montero-Ocampo, C., 2010. Improvement of arsenic electro-removal from underground water by lowering the interference of other ions. Water Air Soil Pollut. 205, 237–244.

Gemici, Ü., Tarcan, G., Helvacı, C., Somay, A.M., 2008. High arsenic and boron concentrations in groundwaters related to mining activity in the Bigadic borate deposits (Western Turkey). Appl. Geochem. 23, 2462–2476.

Goren, A.Y., Kobya, M., 2021. Arsenic removal from groundwater using an aerated electrocoagulation reactor with 3D Al electrodes in the presence of anions. Chemosphere 263, 128253.

Gunduz, O., Simsek, C., Hasozbek, A., 2010. Arsenic pollution in the groundwater of Simav Plain, Turkey: its impacton water quality and human health. Water Air Soil Pollut. 205, 43–62.

Gunduz, O., Bakar, C., Simsek, C., Baba, A., Elci, A., Gurleyuk, H., Mutlu, M., Cakir, A., 2017. The health risk associated with chronic diseases in villages with high arsenic levels in drinking water supplies. Exposur. Health. 9, 261–273.

Gutiérrez, A., Rodríguez, J.F., Castañeda, L.F., Nava, J.L., Coreño, O., Carreño, G., 2022. Abatement of as and hydrated silica from natural groundwater by electrocoagulation in a continuous plant having an electrolyzer and a flocculator-settler. Separ. Purif. Technol. 281, 119895.

Kobya, M., Ulu, F., Gebologlu, U., Demirbas, E., Oncel, M.S., 2011. Treatment of potable water containing low concentration of arsenic with electrocoagulation: different connection modes and Fe–Al electrodes. Separ. Purif. Technol. 77, 283–293.

Kobya, M., Ozyonar, F., Demirbas, E., Sik, E., Oncel, M.S., 2015. Arsenic removal from groundwater of Sivas-Şarkişla Plain, Turkey by electrocoagulation process: comparing with iron plate and ball electrodes. J. Environ. Chem. Eng. 3, 1096–1106.

Kobya, M., Oncel, M.S., Demirbas, E., Celen, M., 2017. Arsenic and boron removal from spring and groundwater samples in boron mining regions of Turkey by electrocoagulation and ion-exchange consecutive processes. Desalination Water Treat. 93, 288–296.

Kobya, M., Omwene, P.I., Sarabi, S.M., Yildirim, S., Ukundimana, Z., 2021. Phosphorous removal from anaerobically digested municipal sludge centrate by an electrocoagulation reactor using metal (Al, Fe and Al-Fe) scrap anodes. Process Saf. Environ. Protect. 152, 188–200.

Lacasa, E., Cañizares, P., Sáez, C., Fernández, F.J., Rodrigo, M.A., 2011. Electrochemical phosphates removal using iron and aluminium electrodes. Chem. Eng. J. 172, 137–143.

Maitlo, H.A., Kim, J.H., Kim, K.H., Park, J.Y., Khan, A., 2019. Metal-air fuel cell electrocoagulation techniques for the treatment of arsenic in water. J. Clean. Prod. 207, 67–84.

Mendoza-Chávez, C.E., Carabin, A., Dirany, A., Drogui, P., Buelna, G., Meza-Montenegro, M.M., Ulloa-Mercado, R.G., Diaz-Tenorio, L.M., Leyva-Soto, L.A., Gortáres-Moroyoqui, P., 2021. Statistical optimization of arsenic removal from synthetic water by electrocoagulation system and its application with real arsenic-polluted groundwater. Environ. Technol. 42, 3463–3474.

Mohora, E., Roncevic, S., Agbaba, J., Zrnic, K., Tubic, A., Dalmacija, B., 2018. Arsenic removal from groundwater by horizontal-flow continuous electrocoagulation (EC) as a standalone process. J. Environ. Chem. Eng. 6, 512–519.

Molgora, C.C., Dominguez, A.M., Avila, E.M., Drogui, P., Buelna, G., 2013. Removal of arsenic from drinking water: a comparative study between electrocoagulation-microfiltration and chemical coagulation-microfiltration processes. Separ. Purif. Technol. 118, 645–651.

Moreno, H.A.C., Cocke, D.L., Gomes, J.A.G., Morkovsky, P., Parga, J.R., Peterson, E., Garcia, C., 2009. Electrochemical reactions for electrocoagulation using iron electrodes. Ind. Eng. Chem. Res. 48, 2275–2282.

Mousazadeh, M., Alizadeh, S.M., Frontistis, Z., Kabdaslı, I., Niaragh, K.E., Al Qodah, Z., Naghdali, Z., Mahmoud, A.E.D., Sandoval, M.A., Butler, E., Emamjomeh, M.M., 2021. Electrocoagulation as a promising defluoridation technology from water: a review of state of the art of removal mechanisms and performance trends. Water 13, 656.

Moussa, D.T., El-Naas, M.H., Nasser, M., Al-Marri, M.J., 2017. A comprehensive review of electrocoagulation for water treatment: potentials and challenges. J. Environ. Manag. 186, 24–41.

Nordstrom, D.K., 2015. Worldwide occurrences of arsenic in groundwater. Science 296, 2143–2145.

Omwene, P.I., Kobya, M., 2018. Treatment of domestic wastewater phosphate by electrocoagulation using Fe and Al electrodes: a comparative study. Process Saf. Environ. Protect. 116, 34–51.

Omwene, P.I., Çelen, M., Öncel, M.S., Kobya, M., 2019. Arsenic removal from naturally arsenic contaminated ground water by packed-bed electrocoagulator using Al and Fe scrap anodes. Process Saf. Environ. Protect. 121, 20–31.

Parga, J.R., Cocke, D.L., Valenzuela, J.L., Gomes, J.A., Kesmez, M., Irwin, G., Moreno, H., Weir, M., 2005. Arsenic Removal via electrocoagulation from heavy metal contaminated groundwater in La Comarca Lagunera Mexico. J. Hazard Mater. 124, 247–254.

Ravenscroft, P., Brammer, H., Richards, K., 2009. Arsenic Pollution: A Global Synthesis, RGS-IBG Book Series. A John Wiley and Sons Ltd. Publication, London.

Sandoval, M.A., Fuentes, R., Thiam, A., Salazar, R., 2021. Arsenic and fluoride removal by electrocoagulation process: a general review. Sci. Total Environ. 753, 142108.

Shen, M., Zhang, Y., Almatrafi, E., Hu, T., Zhou, C., Song, B., Zeng, Z., Zeng, G., 2022. Efficient removal of microplastics from wastewater by an electrocoagulation process. Chem. Eng. J. 428, 131161.

Sık, E., Kobya, M., Demirbas, E., Gengec, E., Oncel, M.S., 2017. Combined effects of co-existing anions on the removal of arsenic from groundwater by electrocoagulation process: optimization through response surface methodology. J. Environ. Chem. Eng. 5, 3792–3802.

Smedley, P.L., Kinniburgh, D.G., 2002. Review of the source, behavior and distribution of arsenic in natural waters. Appl. Geochem. 17, 517–568.

Song, P., Yang, Z., Zeng, G., Yang, X., Xu, H., Wang, L., Xu, R., Xiong, W., Ahmad, K., 2017. Electrocoagulation treatment of arsenic in wastewaters: a comprehensive review. Chem. Eng. J. 317, 707–725.

Sorg, T.J., Wang, L., Chen, A.S.C., 2015. The costs of small drinking water systems removing arsenic from groundwater. J. Water Supply Res. Technol. - Aqua 64 (3), 219–234.

Thakur, L.S., Goyal, H., Mondal, P., 2019. Simultaneous removal of arsenic and fluoride from synthetic solution through continuous electrocoagulation: operating cost and sludge utilization. J. Environ. Chem. Eng. 7, 102829.

Ucar, C., Baskan, M.B., Pala, A., 2013. Arsenic removal from drinking water by electrocoagulation using iron electrodes. Kor. J. Chem. Eng. 30, 1889–1895.

US-EPA (United States-Environmental Protection Agency), 2000. Technologies and Costs for Removal of Arsenic from Drinking Water. EPA/815/R-00/028, Washington.

US-EPA (United States-Environmental Protection Agency), Nov 2, 2016. Drinking water requirements for states and public water systems: arsenic Rule compliance success stories (accessed March 26, 2017). https://www.epa.gov/dwreginfo/arsenic-rule-compliance-success-stories.

Valentín-Reyes, J., Trejo, D.B., Coreño, O., Nava, J.L., 2022. Abatement of hydrated silica, arsenic, and coexisting ions from groundwater by electrocoagulation using iron electrodes. Chemosphere 297, 134144.

Vasudevan, S., Lakshmi, J., Sozhan, G., 2010. Studies relating to removal of arsenate by electrochemical coagulation: optimization kinetics, coagulant characterization. Separ. Sci. Technol. 45, 1313–1325.

Vignesh, A., Siddarth, A.S., Babu, B.R., 2017. Electro-dissolution of metal scrap anodes for nickel ion removal from metal finishing effluent. J. Mater. Cycles Waste Manag. 19, 155–162.

WHO (World Health Organization), 2001. Arsenic in Drinking-Water. World Health Organization, Switzerland-Geneva (Fact Sheet No. 210).

WHO (World Health Organization), 2011. Guidelines for Drinking-Water Quality, fourth ed. WHO, Geneva, Switzerland.

Zhu, J., Zhao, H., Ni, J., 2007. Fluoride distribution in electrocoagulation defluoridation process. Separ. Purif. Technol. 56, 184–191.